Available online at www.sciencedirect.com
ScienceDirect
Journal of Sound and Vibration 323 (2009) 910–931
JOURNAL OF SOUND AND VIBRATION
www.elsevier.com/locate/jsvi

Study of coupled supersonic twin jets of complex geometry using higher-order spectral analysis

K. Srinivasan[a,b], Praveen Panickar[a], Ganesh Raman[a,*], Byung-Hun Kim[a], David R. Williams[a]

[a]*Fluid Dynamics Research Center, Illinois Institute of Technology, 10 W. 32nd Street, Chicago, IL-60616, USA*
[b]*Department of Mechanical Engineering, Indian Institute of Technology Madras, Chennai 600 036, India*

Received 20 September 2006; received in revised form 9 November 2008; accepted 8 January 2009
Handling Editor: C.L. Morfey
Available online 20 February 2009

Abstract

The purpose of this paper is to examine nonlinear processes occurring during the coupling of complex twin jet plumes using higher-order spectral methods. Inadequacies of linear spectral analysis when closely spaced multiple screech sources exist in complex configurations are demonstrated. Cross-bicoherence is used for identifying the nonlinear interactions between jets emanating from rectangular nozzles with spanwise oblique exit geometries. Two basic topologies in twin jets are compared in the paper; one that promotes coupling (referred to as 'co-directed') and another that inhibits coupling (referred to as 'contra-directed'). The primary findings are: (i) some configurations that appeared to be uncoupled by linear spectral analysis metrics were actually found to be nonlinearly coupled, and (ii) two types of nonlinear coupling were observed—one dominated by the fundamental and its interaction with higher modes, and another that displayed clusters of interactions between a frequency component and its sidebands. Further, three new metrics have been proposed: (i) the first metric, 'quadratic phase coupling index', was developed and used to indicate the propensity of jets to couple, (ii) the second metric, namely, 'interaction density' was developed to quantify nonlinear coupling, and (iii) the third metric known as the 'average interaction density' was shown to increase sharply during coupling mode transition.

1. Introduction

1.1. Background

The tandem jet configuration is common in several military aircraft. The interaction between two shock-containing jet plumes in close proximity has been investigated in this work. Such interactions can alter the flow and acoustic field substantially, leading to enhanced acoustic pressures in the near-field. The possibility of structural damage to engine nozzles from such unsteady loads is well known and continues to be of concern to the aircraft industry. Acoustic fields have traditionally been characterized using linear spectral analyses of

*Corresponding author. Tel.: +1 312 567 3554; fax: +1 312 567 7230.
E-mail address: raman@iit.edu (G. Raman).

0022-460X/$ - see front matter © 2009 Elsevier Ltd. All rights reserved.
doi:10.1016/j.jsv.2009.01.011

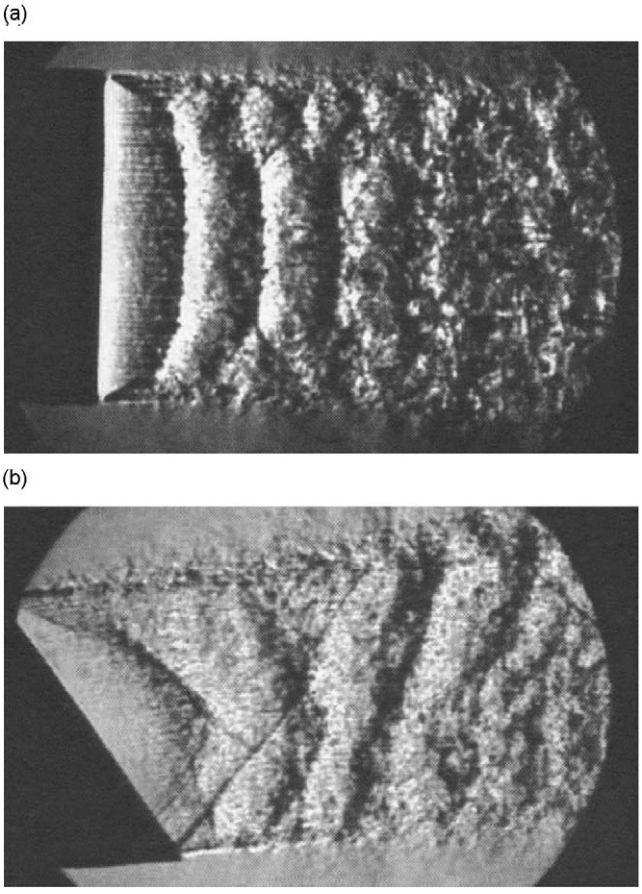

Fig. 1. Shock structures in rectangular nozzles (from Ref. [12]). (a) Uniform rectangular exit and (b) single-beveled exit.

single and two point measurements. These methods are usually adequate to describe acoustic fields comprising a simple acoustic source, or, multiple sources where the spatial separation of acoustic sources is much larger than the characteristic acoustic wavelength. In the case of shock-containing jets, there could be multiple acoustic sources of comparable strengths, spatially separated within a few acoustic wavelengths. There is evidence in the literature of jets with multiple screech tones, with their corresponding feedback loops. When such complexities are possible in a single jet plume (Fig. 1(a)), further complexity is inevitable when the shock-cells are spanwise oblique (Fig. 1(b)) and when another jet is located in close vicinity.

The present study characterizes the acoustic interactions that can occur between tandem jets with complex shock structures, and the rich facet of nonlinearity in jet interactions has been brought out. The subsequent subsections briefly review the literature concerning (a) the acoustics of nozzles with complex geometry, and (b) instances of other flow situations where higher-order spectral analyses have been successfully used.

1.2. Review of relevant literature

Interest in acoustic modes and their coupling in jet flows arose following observations of their undesirable consequences, such as acoustic fatigue damage in laboratory and full-scale tests. Early studies [1–7] were conducted on circular jets in single and twin configurations. Tam and Seiner [8] reported screech frequency variations in twin and single jets. Morris [5] made extensive instability analyses on twin circular jets that corroborated earlier experimental results. Representing the twin jets by two circular vortex sheets, he concluded that the unsteady flow fields interact before the merger of the mean flows. Later, the focus

diversified to rectangular and other non-axisymmetric configurations owing to their aerodynamic, acoustic and stealth benefits [9–16]. The topics of interest in this field of research can be classified as follows:

(a) Characterization of screech in rectangular jets and its effect on flow features like jet mixing, spreading rate, entrainment, and so on. These studies added substantial information to the knowledge base for use in design (see Refs. [10–12]).
(b) Characterization of screech modes, their interactions and effects: These studies aided further insights into the various manifestations of screech and attempted to relate the hydrodynamic instability to the acoustic field (see Refs. [9,10]).
(c) Analytical models for screech prediction: These studies demonstrated that the screech tone could be predicted for non-axisymmetric jets with sufficient accuracy using instability calculations and waveguide approach (see Refs. [17,18]). In the context of the present work, it should be noted that analytical prediction of multiple jets of non-circular exit geometries is still elusive. Analytical treatment becomes more complex when the exit geometries are non-uniform (for e.g., beveled geometries, wherein the shear layers commence from different axial locations of the jet exit device, thus making dispersion relation calculations difficult). Given the fact that even a simple circular jet does not lend itself to screech amplitude predictions, an analytical approach is difficult for uncovering the dynamics of complex plume systems.
(d) Screech studies in complex geometrical situations such as multijets, and the use of passive control devices in the form of structural modifications to the jet exit, vicinity, and so on. For example, answers to some interesting scientific questions such as the possibility of screech synchronization in a multijet situation emerged from these studies. Further, various techniques to avoid screech and its ill effects emerged from this class of studies (see Refs. [1,3,6,11,13–16,19]).

The above classification is by no means exhaustive. Some of the earlier work may overlap two or more areas mentioned above. Nevertheless, the purpose of this classification is to present the present work in the perspective of screech research on rectangular jets. Thus, the current paper may be classified under categories (b) and (d) as an attempt to gain insight into the coupling modes in twin jets. This work further attempts to demonstrate the use and relevance of nonlinear spectral analysis in jet acoustic interactions. Some pertinent earlier studies are presented below to serve as the background for the present work.

Raman and Rice [9] conducted experiments on single rectangular jets to reveal finer details about the instability modes resulting from screech. They reported that in a single rectangular jet, the fundamental screech frequency, f, exhibits an antisymmetric mode while its first harmonic, $2f$, exhibits a symmetric mode. Raman and Taghavi [14] conducted a detailed study of the near acoustic field and the coupling mechanism of twin rectangular supersonic jets having uniform exit geometry. They found that there were two modes of coupling that prevailed—the symmetric mode that augmented the screech amplitude and the antisymmetric mode that suppressed it, and both these modes were mutually exclusive. A companion study by Taghavi and Raman [15] on twin jets having straight rectangular exit geometry in various configurations found that the shock spacing did not change significantly when the jets coupled. The coupling of twin supersonic jets with a double-beveled exit geometry was studied by Raman [11], who found that twin double-beveled jets can couple and may lead to either an augmentation or suppression of sound in the inter-nozzle region depending on the fully expanded Mach number at which the jets were operating. Although previous work has illuminated some aspects of individual single-beveled nozzles [12,20], as well as twin double-beveled nozzles [11], to the best of knowledge of the authors, there is no published information on the interaction between jets from single-beveled nozzles using either linear or nonlinear techniques.

The authors recently conducted experiments on twin single-beveled exit geometry configurations using conventional linear spectral analyses. The earlier work revealed that while the single-beveled jet exhibits spanwise symmetric, spanwise antisymmetric, and spanwise oblique modes while operating individually (Fig. 2(a)), they coupled only in spanwise symmetric and spanwise antisymmetric modes when operated in the twin jet mode.

Such observations about the contrasting behavior of single and twin jets had been made earlier for double-beveled configurations [11]. Further, the coupling in the twin jet was restricted to a configuration wherein the

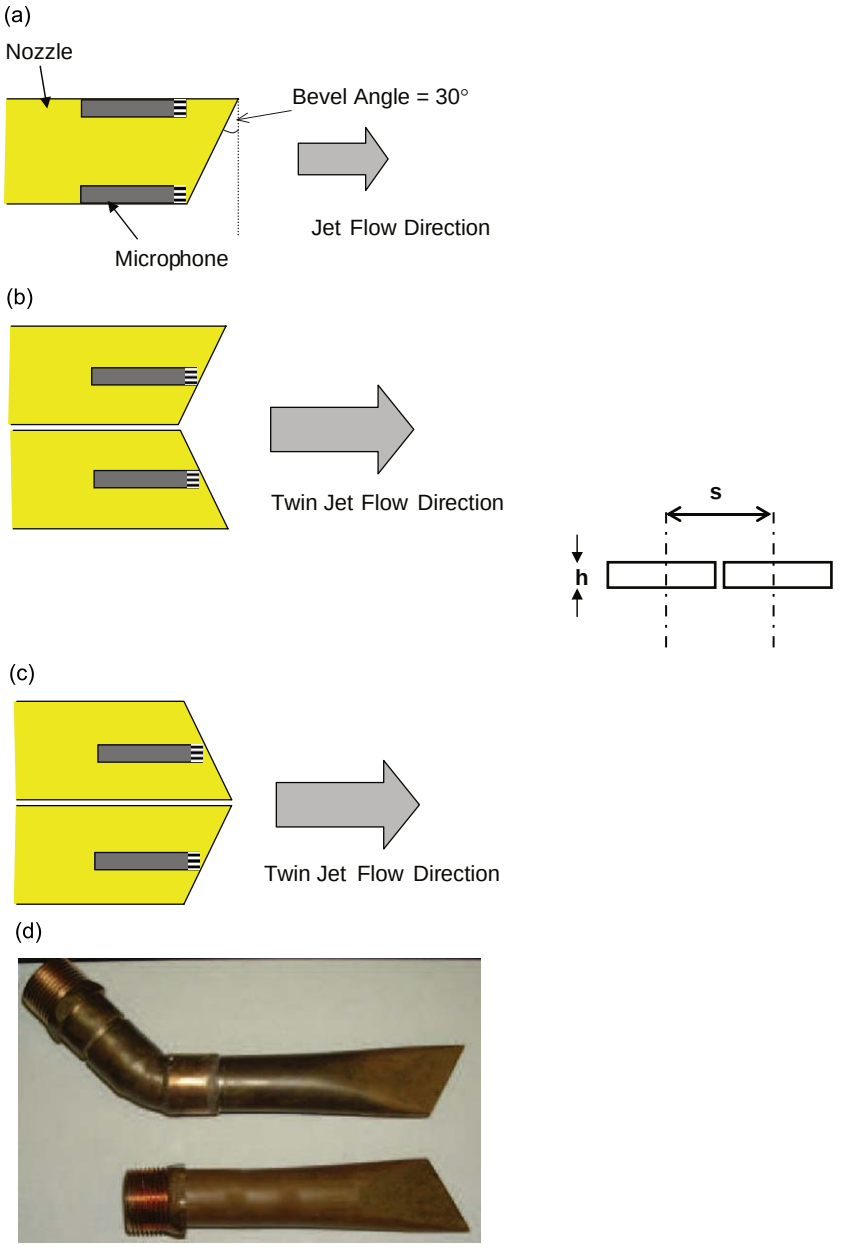

Fig. 2. Single and twin jet configurations studied. Microphone positions are shown against each configuration. (a) Single jet, (b) twin jet: co-directed, (c) twin jet: contra-directed, and (d) photograph of nozzles.

jets were directed towards each other (co-directed) as shown in Fig. 2(b). The other possible twin jet configuration where the jets were directed away from each other (contra-directed) (Fig. 2(c)) did not show coupling behavior. These results were obtained using linear power spectra, spanwise phase measurements and directivity measurements. The curious observation that propelled the authors to use higher-order tools was the fact that at certain geometric and flow conditions, the jets showed frequency locking, but lacked a strong phase coherence. The jets under such conditions were considered 'uncoupled', based on phase coherence. Further, Lissajou plots of the two microphone data suggested the possibility of nonlinearity in the coupling phenomenon.

The justification of the present work stems from the fact that all the previous work had used conventional spectral analysis. Consequently, fundamental explanations to certain interesting observations were not provided in several previous papers. For instance, in the work of Raman and Taghavi [14] one observes the existence of two closely spaced peaks. Questions such as why do two peaks of comparable magnitude appear in the spectrum? Do they have a special phase relationship? Why was this peculiar behavior observed near the coupling mode switching condition? Such features have remained unanswered in the field of aeroacoustics. With the advent of the use of higher-order spectral methods in various physical applications, a fundamental understanding of complex problems seems to be possible.

1.3. Higher-order spectral methods in free shear flows

The higher-order spectral methods were initially used for understanding the nonlinearity in other branches of engineering, such as the electrical sciences, resulting in several useful nonlinear spectral tools (see for instance, Refs. [21,22]). Later, higher-order spectral tools were used to advance the understanding of free shear flows. The need for these tools emerged from the challenge posed by the extensive nonlinearity in the axial evolution of shear layers. The auto-bicoherence and the cross-bicoherence are the nonlinear analogues of the auto-spectrum and cross-spectrum functions in the conventional linear spectral analyses. The auto- and cross-bispectra are the Fourier transforms of triple time correlations of two functions of time, the functions being identical in the case of auto-spectrum. The mathematical form of cross-bispectrum is shown in Eq. (1). The discrete frequency domain form suitable for computations is presented in Section 2:

$$B_{yxx}(f_1,f_2) = \int_{-\infty}^{\infty}\int_{-\infty}^{\infty}\left[\lim_{T\to\infty}\frac{1}{T}\int_0^T y(t)x(t+\tau_1)x(t+\tau_2)\,\mathrm{d}t\right]\exp\{-2\pi(f_1\tau_1+f_2\tau_2)\}\,\mathrm{d}\tau_1\,\mathrm{d}\tau_2. \quad (1)$$

Some earlier work on the use of these techniques in free shear flows is presented below to serve as an example to justify the use of these techniques in the present work. Thomas and Chu [23,24] studied the evolution of a planar shear layer using auto- and cross-bicoherence functions to trace the axial evolution of the planar shear layer. They used time series data from two spatially separated hot-wire probes to perform the nonlinear analysis. The axial location of the probe-pair was varied, and both the linear and the nonlinear spectra were obtained and analyzed. They, inter alia, concluded that the cross-bispectrum was more useful than the auto-bispectrum in space-localizing the nonlinear processes, and observed that the shear layer showed a preference for difference interactions than sum interactions. Thomas and Chu [25,26], extended their work to unravel other interesting dynamics of the shear layer. Using higher-order cumulants, they were able to quantify the significance of nonlinearity by obtaining the linear and nonlinear coupling coefficients. These studies revealed the role of resonance involving subharmonics on the shear layer development.

Higher-order spectral analysis was first used in the study of high speed flows by Ponton and Seiner [7] and by Walker and Thomas [27]. Ponton and Seiner [7] conducted extensive time-series analysis as well as linear and nonlinear spectral analysis on a choked circular jet. They used an azimuthal array of microphones and performed time-series analysis to uncover the physics of the helical mode of the jet instability. They found that the flapping plane of the jet rotated azimuthally in a random fashion. They also presented auto-bicoherence for the microphone signal with which they were able to identify the nonlinear interactions. Walker and Thomas [27] conducted experiments on screeching rectangular jets. They demonstrated that while linear techniques such as spectra, SPL contours, phase coherence provide valuable information about the gross features of a screeching jet, the nonlinear wave interactions can be identified only by nonlinear spectral methods. They used nonlinear spectra to quantify the quadratic interactions. Their results obtained from a hydrodynamic analysis were consistent with their acoustic studies, emphasizing the direct correspondence between the two. They were able to deduce the interactions between the various modes using nonlinear spectra, and trace the axial evolution of each mode.

Although the present paper involves screeching jets, the focus is different. Rather than individual jet modes, twin jet coupling modes are addressed. The objectives of the present work are outlined in detail in the following section.

1.4. Objectives of the present work

The focus of this paper is to study twin rectangular jets of complex geometry, and to study their coupling behavior using higher-order spectral properties such as cross-bicoherence. The work attempts to quantify nonlinear interactions occurring in these jets and relate them to the power spectra and jet coupling behavior. It should be noted that nonlinear interactions are manifestations of the nonlinear flow physics in the jet plumes and do not involve nonlinear acoustics. It is assumed that the hydrodynamic sources are nonlinear, and the signatures of these nonlinear processes are measured in the near field.

To accomplish these objectives, three basic configurations were chosen: (i) twin jets directed towards each other (co-directed), (ii) twin jets directed away from each other (contra-directed), and (iii) single jet. The dimensions of individual nozzles were 35.56 mm in the spanwise direction and 5.08 mm in the transverse direction. Thus, the aspect ratio of the individual jets was 7. The fully expanded Mach number range covered in the study was $1.30 \leqslant M_j \leqslant 1.51$, beyond which the jets did not screech. The inter-nozzle spacing was varied in the co-directed twin jet configuration over the range $7.3 \leqslant s/h \leqslant 7.9$, where s and h are nozzle center spacing and height as indicated in Fig. 2. The inter-nozzle spacing was not varied in the contra-directed configuration since it did not show coupling.

Two microphones were placed at the respective spanwise centers of the nozzles, so as to detect the spanwise coupling behavior. The distance between the two microphone locations was the same as the inter-nozzle distance, and was of the order of a screech wavelength. As observed earlier [9] in the case of large aspect ratio rectangular jets, the jets showed antisymmetric mode instability in the transverse direction.

The experiments were carried out in the high speed jet facility at the Illinois Institute of Technology. The test facility details are described in Panickar et al. [28]. All acoustic measurements were made using 6.35 mm ($\frac{1}{4}$ in) diameter Brüel & Kjær microphones (model 4939), and the microphone locations are shown in Fig. 2. These microphones have a flat response up to 100 kHz within ±3 dB, and within ±1 dB for the frequency range used in the present work. All the data acquisition was achieved using a PC based National Instruments data acquisition board (Model NI PCI-MIO-16E-1) capable of acquiring 1.25 megasamples/s interfaced using LabVIEW 6*i*. The uncertainty in the sound pressure is within ±1 dB, and that in the frequency is within 100 Hz. The data were analyzed using MATLAB 6.5 to yield power spectra and cross-bicoherence. The nonlinear tool used is discussed in Section 2, and results of nonlinear spectral analyses are presented in Section 3.

2. Computation of cross-bicoherence

Cross-bicoherence is a third-order estimate obtained from two simultaneously acquired time-series signals. The third-order bispectrum and bicoherence are computed from the Fourier transform of the triple correlation of the time-series signals, as mentioned earlier. Cross-bicoherence is the normalized cross-bispectrum. The discrete cross-bispectrum is expressed for an ensemble as

$$S^{(k)}_{YXX}(f_1,f_2) = Y^{(k)}(f_1+f_2)X^{(k)*}(f_1)X^{(k)*}(f_2), \tag{2}$$

where $X^{(k)}(f)$ and $Y^{(k)}(f)$ are the DFT of discrete time-series signals $x(t)$ and $y(t)$, and the asterisk $(*)$ represents the complex conjugate. An average is done over M ensembles to obtain the final estimate of discrete cross-bispectrum as

$$S_{YXX}(f_1,f_2) = \frac{1}{M}\sum_{k=1}^{M} S^{(k)}_{YXX}(f_1,f_2). \tag{3}$$

The cross-bicoherence spectrum is then obtained by normalizing this quantity with the power spectra of the two signals as follows:

$$b_c^2(f_1,f_2) = \frac{|S_{YXX}(f_1,f_2)|^2}{\left(\sum_{k=1}^{M}|Y^{(k)}(f_1+f_2)|^2\right)\left(\sum_{k=1}^{M}|X^{(k)}(f_1)X^{(k)}(f_2)|^2\right)}. \tag{4}$$

The computation of these quantities is simplified by using symmetry properties in the frequency domain. An example demonstrating the use of cross-bicoherence is presented in the following paragraph.

Referring to Eqs. (2)–(4), the interaction corresponding to a frequency pair (f_1, f_2) is termed either as a 'sum interaction' or as a 'difference interaction', depending on whether f_1 and f_2 have the same, or the opposite signs. Sum and difference interactions between signals and the ability of cross-bicoherence to discriminate between them can be illustrated by generating two sinusoids as follows:

$$f(t) = \sin(\omega_1 t) + \sin(\omega_2 t) \tag{5}$$

and

$$g(t) = \sin(\omega_1 t)\sin(\omega_2 t + \varepsilon\,\mathrm{rand}\,(t)), \tag{6}$$

where ω_1 and ω_2 are the circular frequencies, and ε rand (t), added as a phase component in one of the sinusoids, is a time varying random number with zero-mean and standard deviation ε $(0 \leqslant \varepsilon \leqslant 0.1)$. The phase randomness simulates noise in experiments that is often referred to as phase jitter.

These two signals are used as inputs to the program that computes the cross-bicoherence spectrum. The linear power spectra of the signals are shown in Fig. 3(a), and cross-bicoherence spectrum is shown in Fig. 3(b). In Fig. 3(b), only the region bounded by the two 45° lines in the upper half-plane, and that in the lower half-plane are unique. Exploiting these symmetry properties, the computation is restricted to this region. Note that in this example, the two sinusoids have frequencies of $f_1 = 5\,\mathrm{kHz}$ and $f_2 = 8\,\mathrm{kHz}$. It can be seen

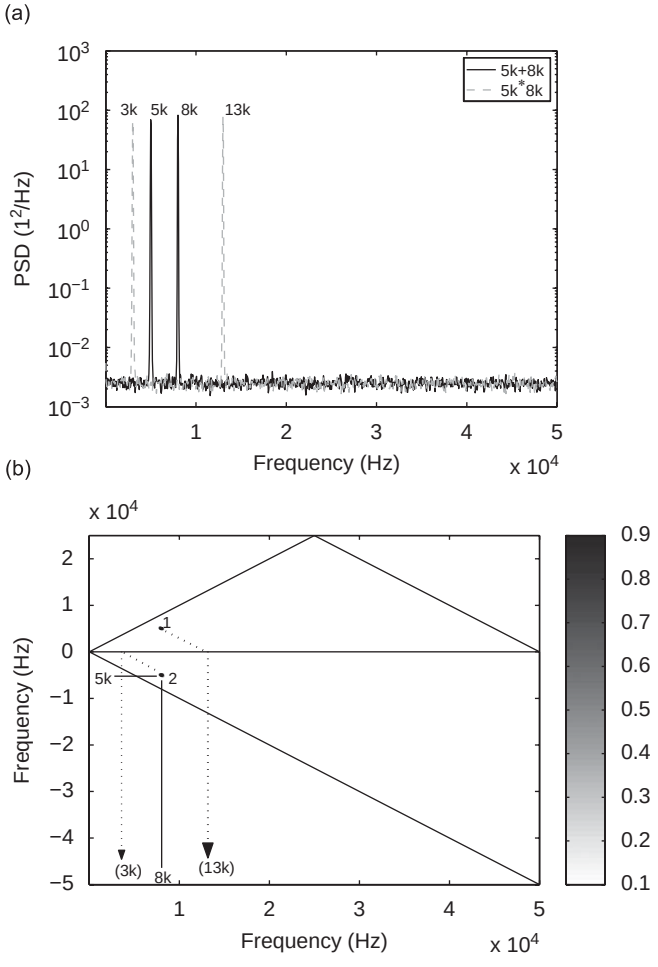

Fig. 3. Linear and nonlinear spectra of test signals. (a) Conventional power spectra and (b) cross-bicoherence spectra.

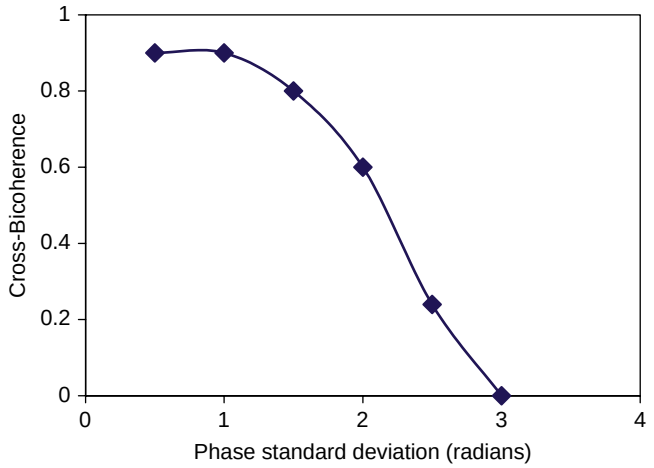

Fig. 4. Sensitivity of cross-bicoherence to phase standard deviation between modulated test sinusoids.

that the cross-bicoherence spectrum shows two distinct peaks; one at the sum interaction position at (f_1,f_2), where $b_c^2(8\,\text{kHz}, 5\,\text{kHz}) = 0.9$ and the other at the difference interaction position at $(f_1,-f_2)$, where $b_c^2(8\,\text{kHz}, -5\,\text{kHz}) = 0.9$, indicating the presence of the frequencies f_1+f_2, and f_1-f_2, respectively, in the modulated signal. Hence, the advantage of cross-bicoherence is its ability to identify such nonlinear interactions, which is not possible with second-order methods such as power spectra.

It is necessary for the phase standard deviation ε between the two signals to be small for the cross-bicoherence to be detectable. The effect of ε is studied by computing the cross-bicoherence for various values of ε in Eq. (6). The variation of the peak cross-bicoherence between the above test signals and the relative phase standard deviation between the modulated signals is plotted in Fig. 4. The number of ensembles used to compute the cross-bicoherence is about 200. This plot shows that the cross-bicoherence is unchanged for small random phase standard deviations, but drops significantly beyond a value of around $\pi/2$.

The twin jet time-series data obtained over a parametric range comprising Mach number and inter-nozzle spacing were analyzed and the results are presented in the subsequent section.

3. Results of nonlinear spectral analyses

Time-series data were acquired from the two microphones for 15 Mach numbers, for the six geometric configurations considered in this study. For each set of time-series data, the power spectrum was computed resulting in 180 power spectra. Further, each pair of time-series data resulted in a cross-bicoherence spectrum. Therefore, owing to the volume of the data, only a few comparisons are being presented. It was shown by Thomas and Chu [25] that the local coherency property of the cross-bicoherence measurement allows the linear and quadratic mechanisms to be quantified. If only a single sensor is used, or if the spacing between the two sensors is greater than the wavelength of interacting modes, then ambiguity arises in the bispectrum. The conditions for 'local coherency' were not met in this experiment for frequencies greater than 1.3 kHz, therefore no attempt was made to quantify the linear and quadratic mechanisms contributing to the cross-bicoherence measurement. Here, the main focus is to clarify the manifestation of nonlinearity in various situations, and answer the following questions:

(a) How do flow and geometrical parameters influence nonlinearity?
(b) Are there patterns in the nonlinear interaction set that would enable the classification of various interaction types?
(c) Is it possible to quantify the nonlinear interactions by identifying pertinent metrics?

These issues are addressed by comparing two twin jet configurations; one that showed coupling (co-directed), and the other that did not couple (contra-directed).

3.1. Co-directed and contra-directed configurations

Fig. 5 compares the cross-bicoherence spectra and power spectra for the co-directed and contra-directed twin jets. There are numerous peaks in the 3-D cross-bicoherence plots, indicative of quadratic phase coupling between the corresponding modes. It may be observed that the maximum value of cross-bicoherence for the

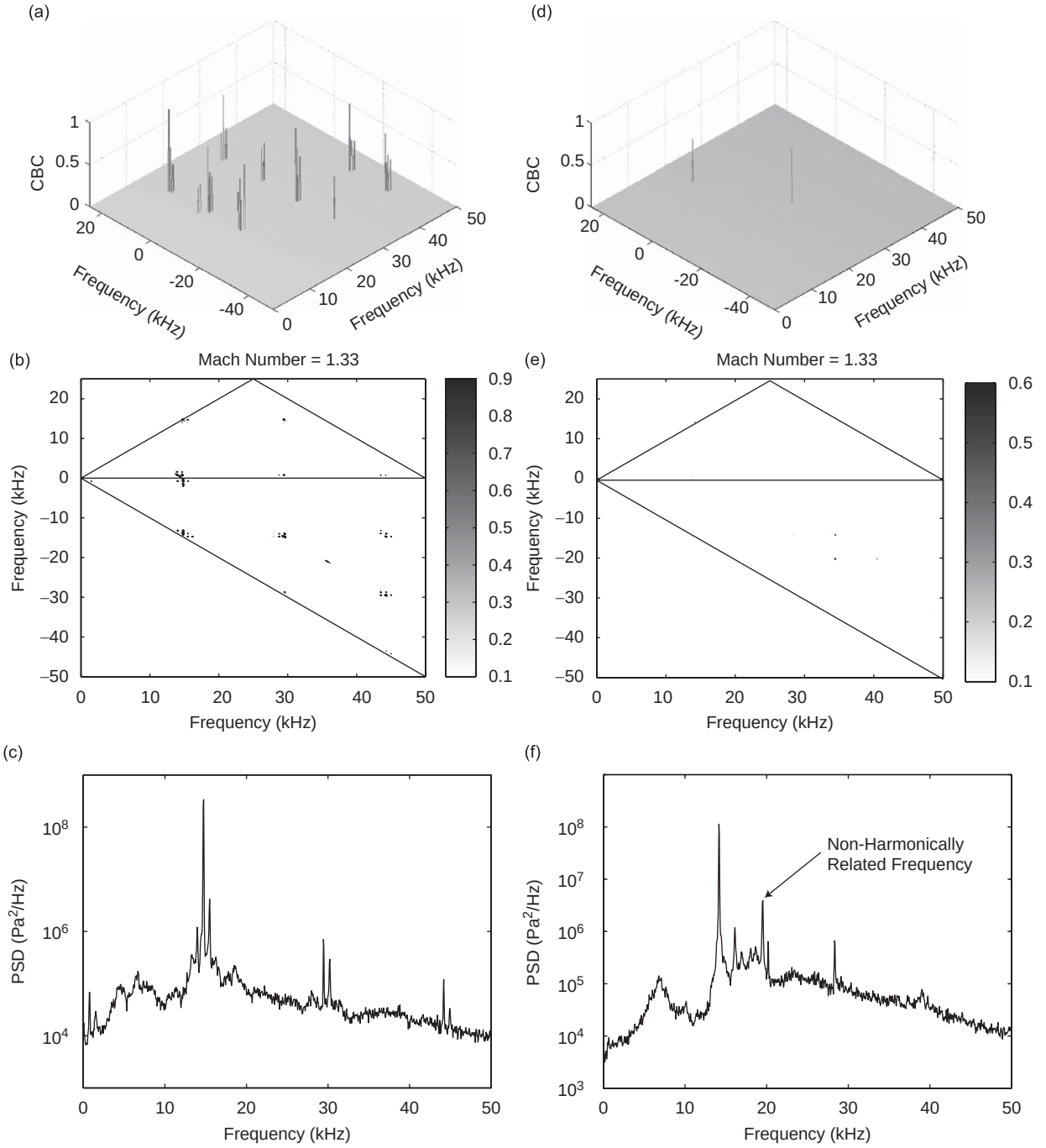

Fig. 5. Cross-bicoherence and spectra of twin jets at $M_j = 1.33$, $s/h = 7.3$ for co-directed and contra-directed configurations. (a,b) Cross-bicoherence spectrum for co-directed configuration, (c) linear power spectrum for co-directed configuration, (d,e) cross-bicoherence spectrum for contra-directed configuration, and (f) power spectrum for contra-directed configuration.

co-directed jets (0.9) is much higher than that for the contra-directed jets (0.6). These observations add further insights to the earlier results obtained through linear phase coherence measurements which showed that while the co-directed configuration coupled, the contra-directed configuration did not couple at all. Therefore, it is possible that there is a stronger interaction between the instabilities of the two jets in the co-directed configuration, which, in turn, promotes the occurrence of nonlinear interactions between them. In this context, the results concerning the phase dependence of cross-bicoherence may be recollected, wherein it was mentioned that the phase standard deviation between interacting waves should be small to produce noticeable nonlinear interactions. In the case of the contra-directed configuration, it can be expected that the sound sources in the two jets are farther apart compared to the co-directed jet, and thus acquire a larger phase standard deviation before any interaction could occur. So, the absence of quadratic phase coupling in the case of contra-directed jets is because of larger phase standard deviation attained before interaction between individual sound sources. Another interesting observation is the presence of non-harmonically related frequencies in the linear spectra of both co- and contra-directed jet cases, suggesting that the presence of non-harmonically related frequencies is not necessarily a cause or an effect of nonlinear interactions.

3.2. Comparison of single and twin jets

The nonlinearity in single jets can be compared against that of twin jets with the aid of two parameters: (i) the number of interactions, and (ii) magnitude of interactions, as quantified by the cross-bicoherence. The cross-bicoherence spectra for single and twin jets (Fig. 6) over the entire Mach number range considered in the present study revealed the following: (a) the number of interactions in the single jet is lower than that for twin jets for most of the Mach numbers. At a few Mach numbers, they are almost equal, and (b) the magnitude of the interactions is always greater in the twin jets compared to single jets. This could be due to the fact that in a single jet, the sources are spaced approximately one shock spacing apart, whereas in twin jets, the sources are closer. However, the common features shared by the two cases are that (a) the maximum coherence corresponds to the self-interaction of the screech mode, (b) the screech tone self-interacts to produce the first harmonic, and (c) the first harmonic interacts with the fundamental to produce the second harmonic in the sum interaction, and the fundamental through a difference interaction. The nonlinear interactions in the single jet are quantified in order to relate them to twin jet coupling, as described in the following paragraph.

In order to quantify the quadratic phase coupling in the single jet, a metric called *Quadratic Phase Coupling Index* (*QPCI*) is defined as follows:

$$QPCI_n = \sum_{i=1}^{N}\sum_{j=1}^{M}\alpha(i,j), \quad \alpha(i,j) = \begin{cases} 1, & b_c^2(f_i,f_j) \geqslant n, \\ 0, & b_c^2(f_i,f_j) < n, \end{cases} \tag{7}$$

where N and M are the number of discrete frequency ranges in the cross-bicoherence spectrum. In Eq. (7), n is the cross-bicoherence threshold below which the uncertainties may clutter the analysis. The purpose of introducing this metric is to examine if the single jet nonlinearity offers any clues about the twin jet coupling. The variation of $QPCI_{0.3}$ with Mach number has been shown for single jet in Fig. 7. It is observed that this metric shows a peak for the single jet case at a Mach number of 1.33, at which the twin jets coupled in the symmetric mode. Similarly, the $QPCI_{0.3}$ shows another (smaller) peak around $M_j = 1.4$, at which the twin jets switched from symmetric to antisymmetric mode. This shows that this metric adequately quantifies the propensity of jets to couple, provided other conditions are favorable.

3.3. Effect of Mach number

Fig. 8 shows the variation in the linear and the nonlinear spectra for fully expanded jet Mach numbers $M_j = 1.3$ and 1.46. At lower Mach numbers of the screeching regime, a clustered pattern of interactions is observable. The term 'cluster' refers to closely spaced interactions seen as a bunch of dots in the cross-bicoherence contour plot, as seen in Fig. 8(b).

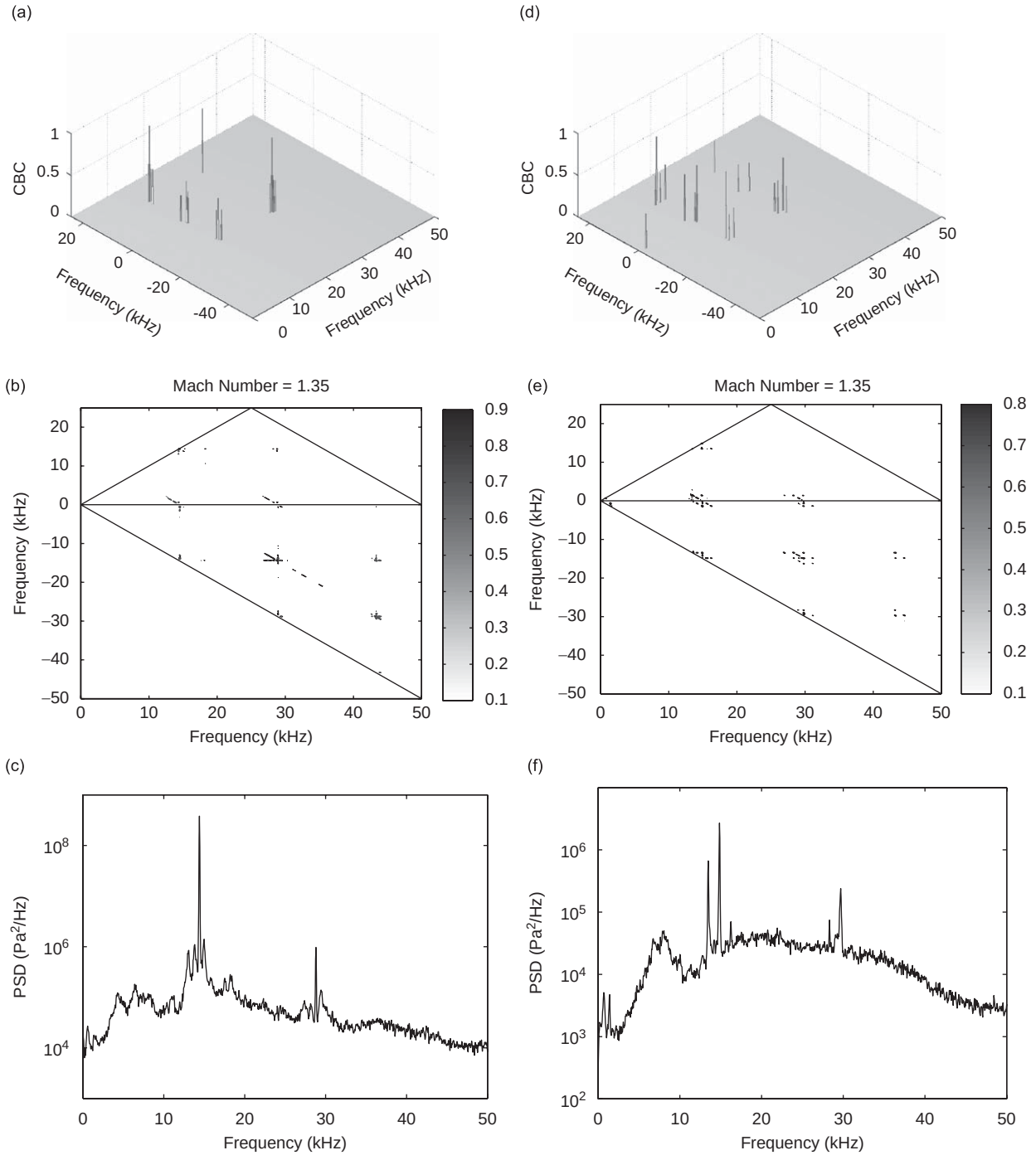

Fig. 6. Comparison of cross-bicoherence spectra and linear power spectra of (a–c) co-directed twin jet and (d–f) single jet. $M_j = 1.35$, $s/h = 7.3$.

The formation of clustered interactions can be explained using Fig. 9. Mode f_1 interacts with a low frequency mode Δf, leading to the formation of $(f_1 + \Delta f)$ and $(f_1 - \Delta f)$. This forms two closely spaced points (separated by frequency $2\Delta f$). These resultant modes then again interact with parent mode Δf leading to the formation of $(f_1 + 2\Delta f)$ and (f_1). Thus, several interactions can exist at closely spaced frequencies. However,

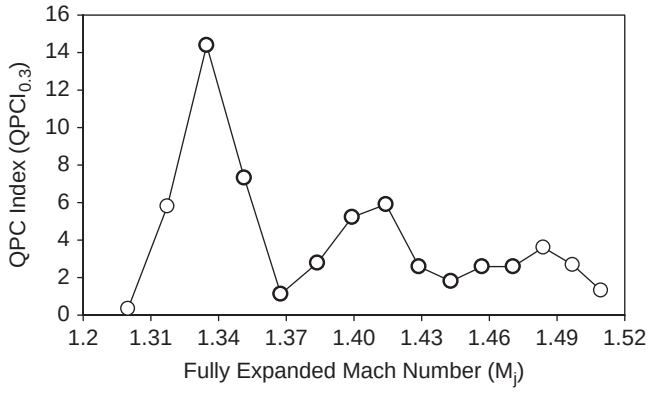

Fig. 7. Variation of *Quadratic Phase Coupling Index* (*QPCI*) with Mach number for the single jet.

this tendency would not continue indefinitely, since this would result in an infinite number of closely spaced points. This is because with each interaction the phase coherency between the participating modes decreases, thereby diminishing the ability to interact.

A close-up view of a cluster is shown in Fig. 10. The sequence of events forming this cluster can be described as follows: Modes f_1 and f_2 interact in a sum interaction to produce the mode (f_1+f_2) (S1 in Fig. 10), and in a difference interaction to produce the mode (f_1-f_2), (D1 in Fig. 10). This is represented by (S1, D1); $b_c^2(f_1,f_2)=0.7$, $b_c^2(f_1,-f_2)=0.7$. The mode (f_1-f_2) participates with mode f_2 to produce a sum mode f_1 with $b_c^2(f_1-f_2,f_2)=0.7$, and a difference mode f_1-2f_2 with $b_c^2(f_1-f_2,-f_2)=0.5$. This mode f_1-2f_2 undergoes a sum interaction with f_2 to yield f_1-f_2 with $b_c^2(f_1-2f_2,f_2)=0.6$. The earlier mentioned resultant mode (f_1+f_2) (S1 in Fig. 10) interacts with f_2 in a difference mode yielding the mode f_1, with $b_c^2(f_1+f_2,-f_2)=0.5$.

The sequences of these interactions have been presented in a binary-tree-like structure in Fig. 11, which describes the hierarchy of modal evolutions. It is interesting to note that as one proceeds down the tree, the cross-bicoherence magnitudes keep decreasing, pointing to the fact that the phase randomness increases with each successive interaction. As Mach number increases, clustering behavior is dominant, except at $M_j=1.33$ which showed the strongest symmetric coupling, where clustering tends to decrease. Beyond the symmetric coupling point, clustering again increases until $M_j=1.4$, where the coupling switched to antisymmetric. In fact, clustering phenomenon is maximum at this 'coupling-transition' Mach number.

The possibility of relating the coupling-transition Mach number with the bevel angle of the nozzle was also examined. The bevel angle in the present case is 30°, and thus the bevel plane makes an angle of 60° with the flow direction. There was no relationship between the wave angle $[\sin^{-1}(1/M_j)]$ of the coupling-transition Mach number and the bevel geometry.

At the antisymmetrically coupled Mach numbers, the clustering phenomenon does not occur (Fig. 8(d–f)), and interactions occur mainly involving the screech frequency and its first harmonic. Thus, from the above observations, it may be stated that the twin jet coupling undergoes a marked variation in nonlinear coupling behavior, with Mach number. It should be pointed out that the clusters observed in the bicoherence spectra are not due to the numerical implementation effects such as FFT record length or number of averages. This was verified by using various combinations of record length and number of averages.

In order to bring out some of the aspects discussed above, details of the major interactions corresponding to Fig. 8(a), are listed in Table 1. It can be seen that the nonlinear interactions are the most energetic (e.g., $b_c^2=0.8$ for interaction 1) when the fundamental mode or the first harmonic mode is involved. It may also be seen that interactions lower in the evolution hierarchy possess a smaller value of cross-bicoherence.

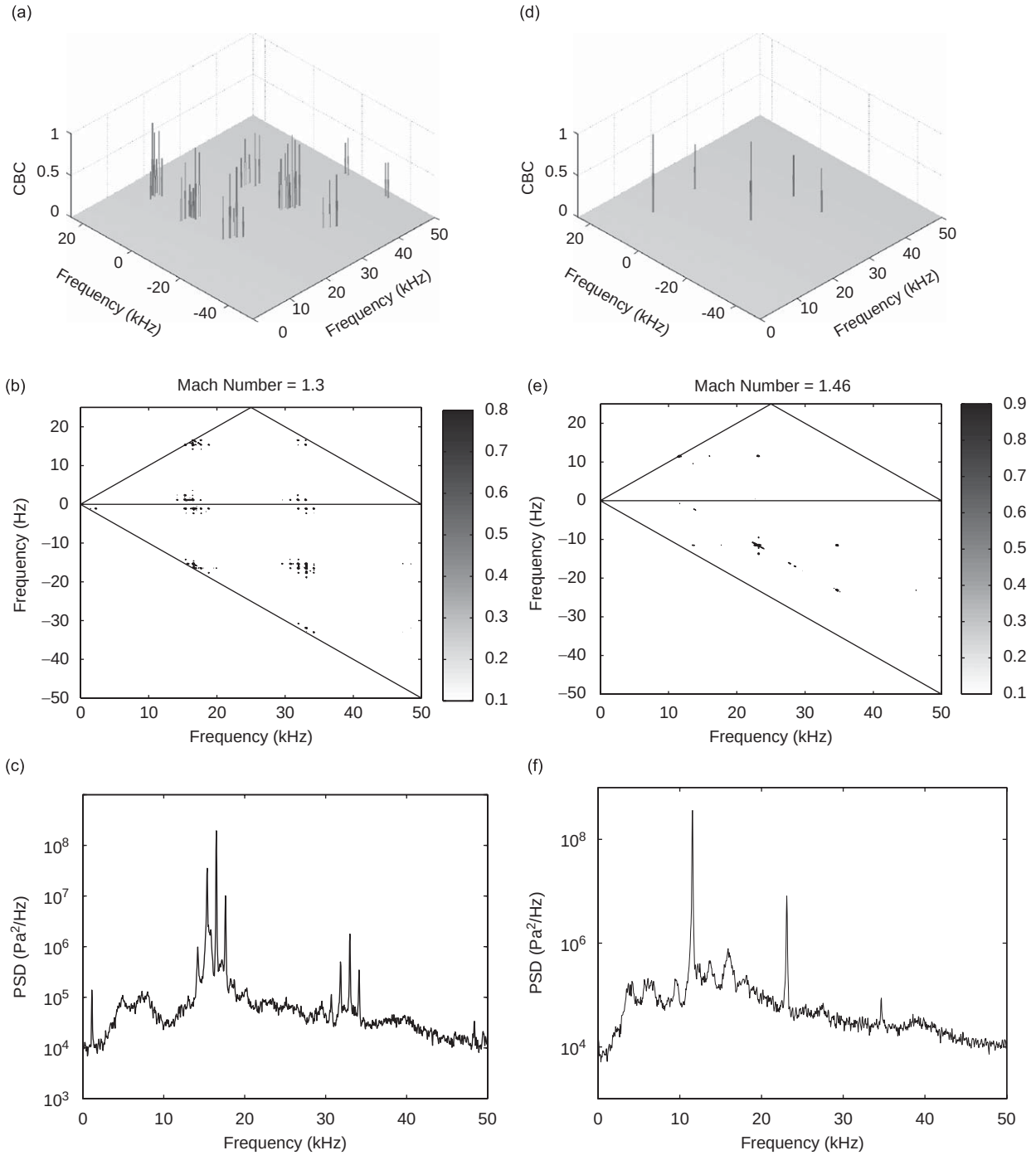

Fig. 8. Cross-bicoherence (3-D and contour plots) and linear spectra of co-directed twin jets at $s/h = 7.3$, for various Mach numbers. (a–c) $M_j = 1.3$ and (d–f) $M_j = 1.46$.

3.4. Effects of inter-nozzle spacing

Fig. 12 compares the effect of inter-nozzle spacing on the nonlinear interactions in co-directed twin jet configurations at $M_j = 1.32$. As can be seen from the figures, the cross-bicoherence spectra show localized clusters in each case. The cluster size grows as inter-nozzle spacing is increased.

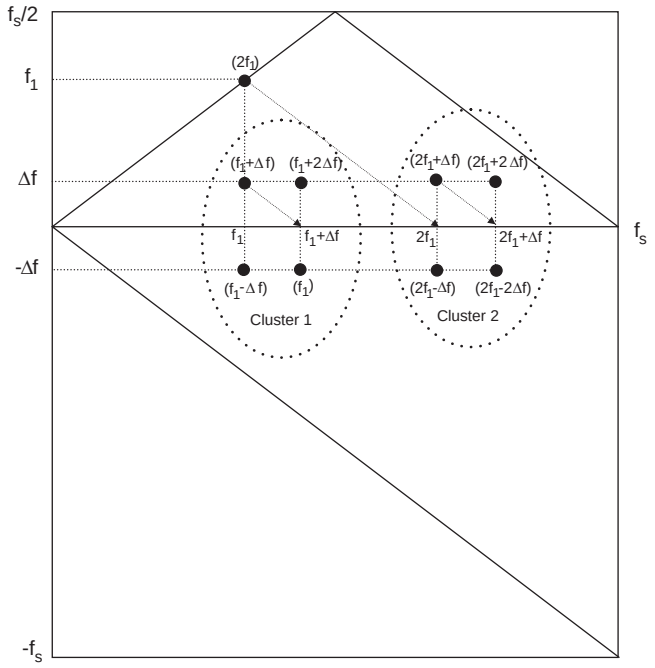

Fig. 9. Depiction of the clustering phenomenon. Frequencies within parentheses denote resultant frequencies, and those without parentheses denote participating frequencies. The dotted ellipses are shown to indicate clusters.

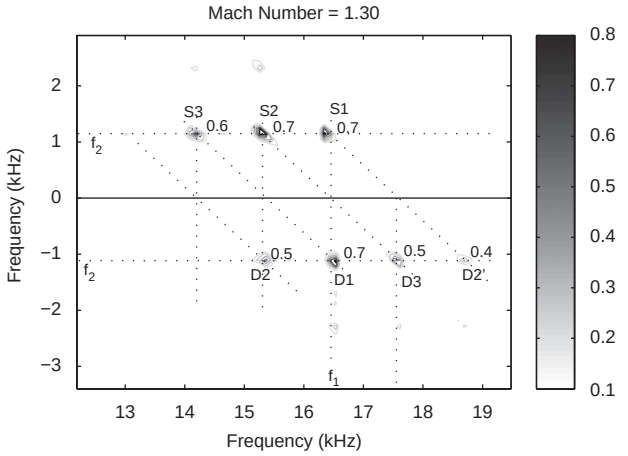

Fig. 10. Close-up view of a cluster illustrating the sequence of interactions building it.

The clusters are mostly located around the fundamental frequency, first harmonic, and the second harmonic. There are other prominent zones, but the aforementioned zones contain relatively higher levels of cross-bicoherence ($b_c^2 > 0.7$). It should be pointed out again that the linear spectra are qualitatively similar to one another. Therefore, it appears that an increase in inter-nozzle spacing promotes nonlinearity. However, there should be a limiting case, since as $s/h \to \infty$, logically, the phase correspondence would be lost, the interactions would lose strength, and the cross-bicoherence would decrease and tend to zero. This was partly verified by obtaining the cross-bicoherence spectrum at an inter-nozzle spacing of $s/h = 11.2$ and $M_j = 1.32$, wherein the interaction density dropped significantly, and the peak cross-bicoherence was relatively low (0.6) (see Fig. 13). From these results it is also obvious that the nonlinearity should peak somewhere in the range where $7.9 < s/h < 11.2$.

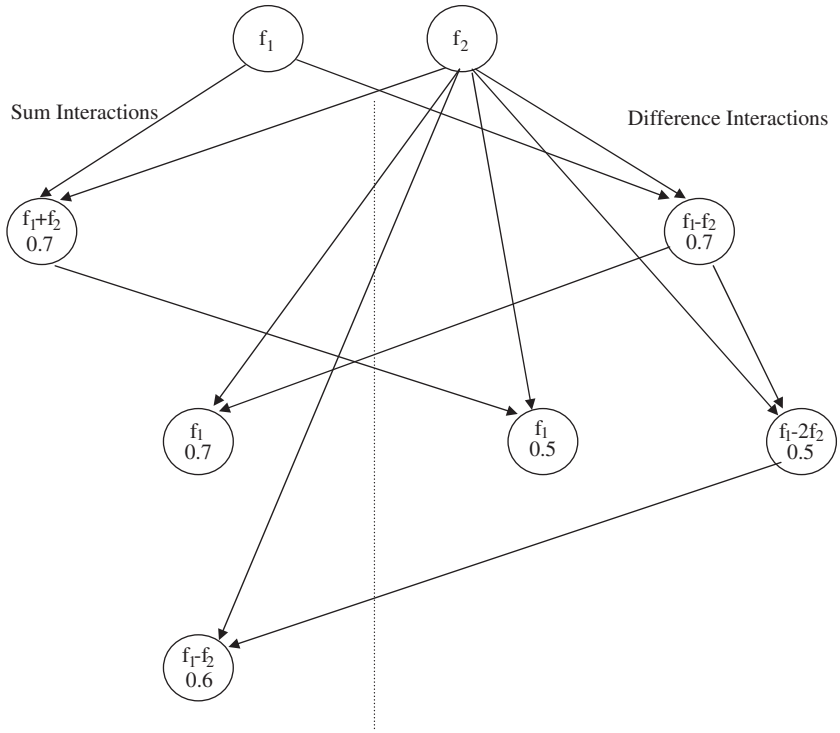

Fig. 11. Details of the evolution of nonlinear interactions shown in Fig. 8. Left-hand side of the illustration shows sum interactions while the right side shows difference interactions. The modes resulting from the interactions are shown inside the circles, and the cross-bicoherence values are mentioned below them.

Table 1
Details of the major nonlinear interactions occurring in the co-directed twin jet at $M_j = 1.3$ and $s/h = 7.3$.

No.	Description of the interaction	$f_{resultant}$ (kHz)	b_c^2
1.	Self-interaction of the fundamental	33	0.8
2.	Difference interaction of 33 and 16.5 kHz	16.6	0.8
3.	Difference interaction of 33 and 17.6 kHz	15.4	0.8
4.	Difference interaction of 17.6 and 16.5 kHz	1.2	0.8
5.	Sum interaction of 17.6 and 15.4 kHz	33	0.7
6.	Sum interaction of 16.5 and 15.4 kHz	31.9	0.7
7.	Difference interaction of 34.1 and 17.6 kHz	16.6	0.7
8.	Difference interaction of 31.9 and 16.5 kHz	15.4	0.7
9.	Difference interaction of 16.6 and 15.4 kHz	1.2	0.7
10.	Difference interaction of 31.9 and 15.4 kHz	16.6	0.6
11.	Sum interaction of 15.4 and 1.1 kHz	16.5	0.6
12.	Difference interaction of 30.7 and 15.4 kHz	15.3	0.6
13.	Difference interaction of 34.2 and 33 kHz	1.2	0.6
14.	Sum interaction of 14.2 and 1.1 kHz	15.4	0.5
15.	Sum interaction of 17.6 and 16.5 kHz	34.1	0.4

Another comparison bringing out the effect of inter-nozzle spacing is presented in Fig. 14, for a slightly higher Mach number of $M_j = 1.46$. The clusters seen in Fig. 12 are no longer seen in this figure, since the necessary low frequency modes do not exist in the spectra. Instead, the interaction is restricted to the self-interaction of the fundamental screech frequency. Another contrasting observation is the presence of

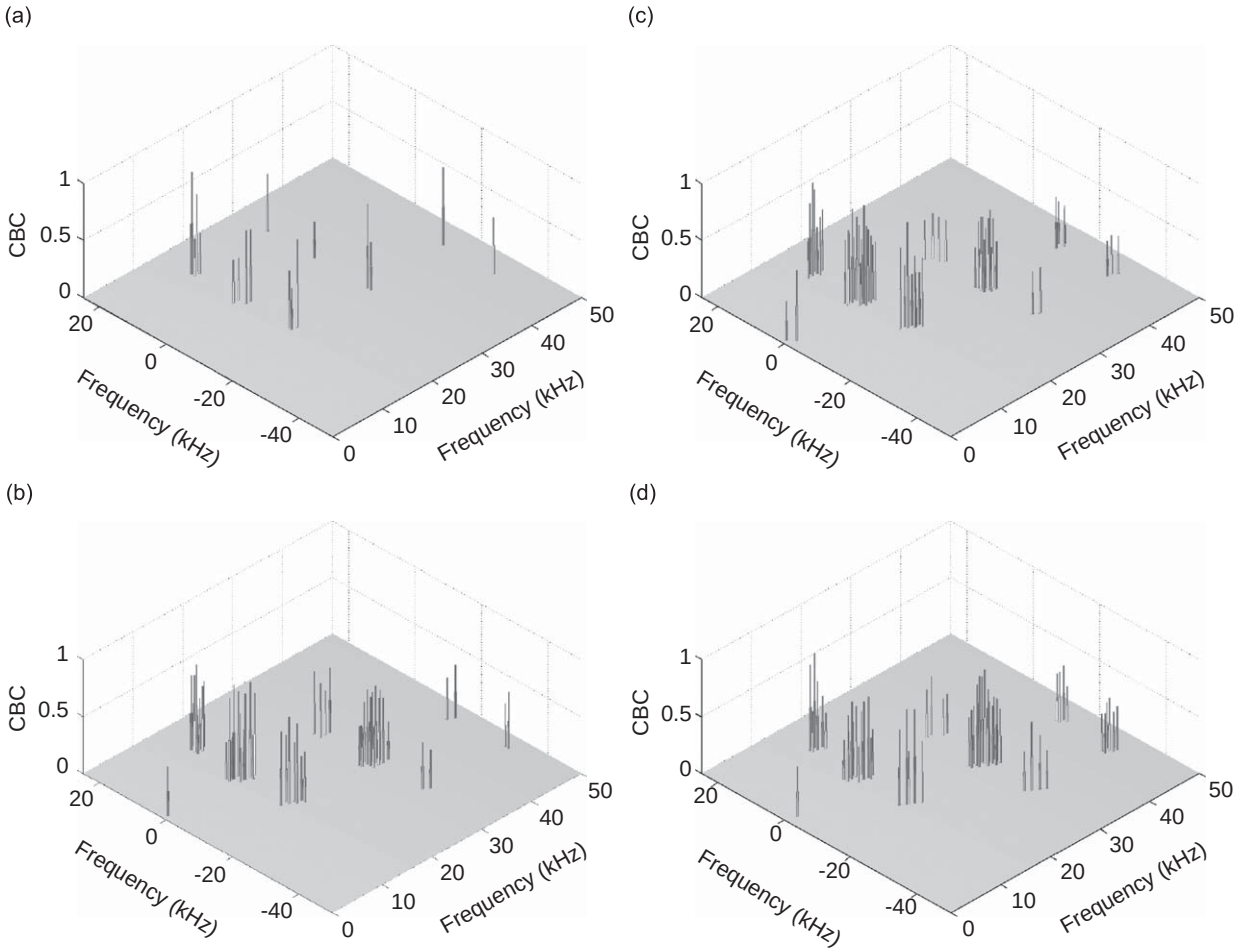

Fig. 12. Cross-bicoherence and spectra of co-directed twin jets at $M_j = 1.32$, for various inter-nozzle spacings. (a) $s/h = 7.3$, (b) $s/h = 7.5$, (c) $s/h = 7.7$, and (d) $s/h = 7.9$.

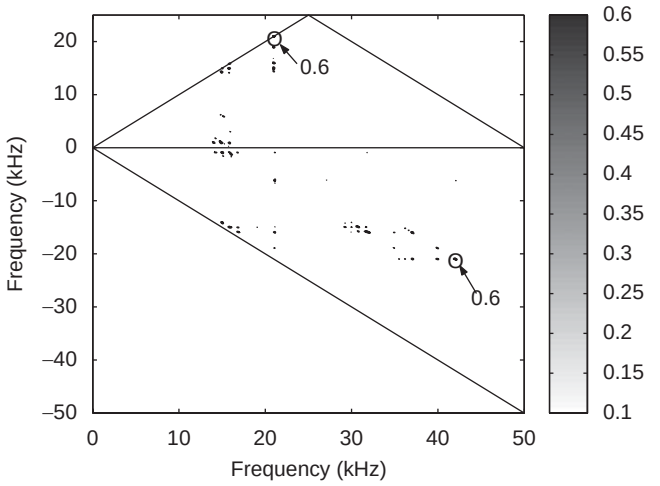

Fig. 13. Cross-bicoherence spectrum of co-directed twin jets at $M_j = 1.32$, and $s/h = 11.2$. Arrow marked interactions had a coherency of 0.6. Other interactions had a coherency between 0.3 and 0.6.

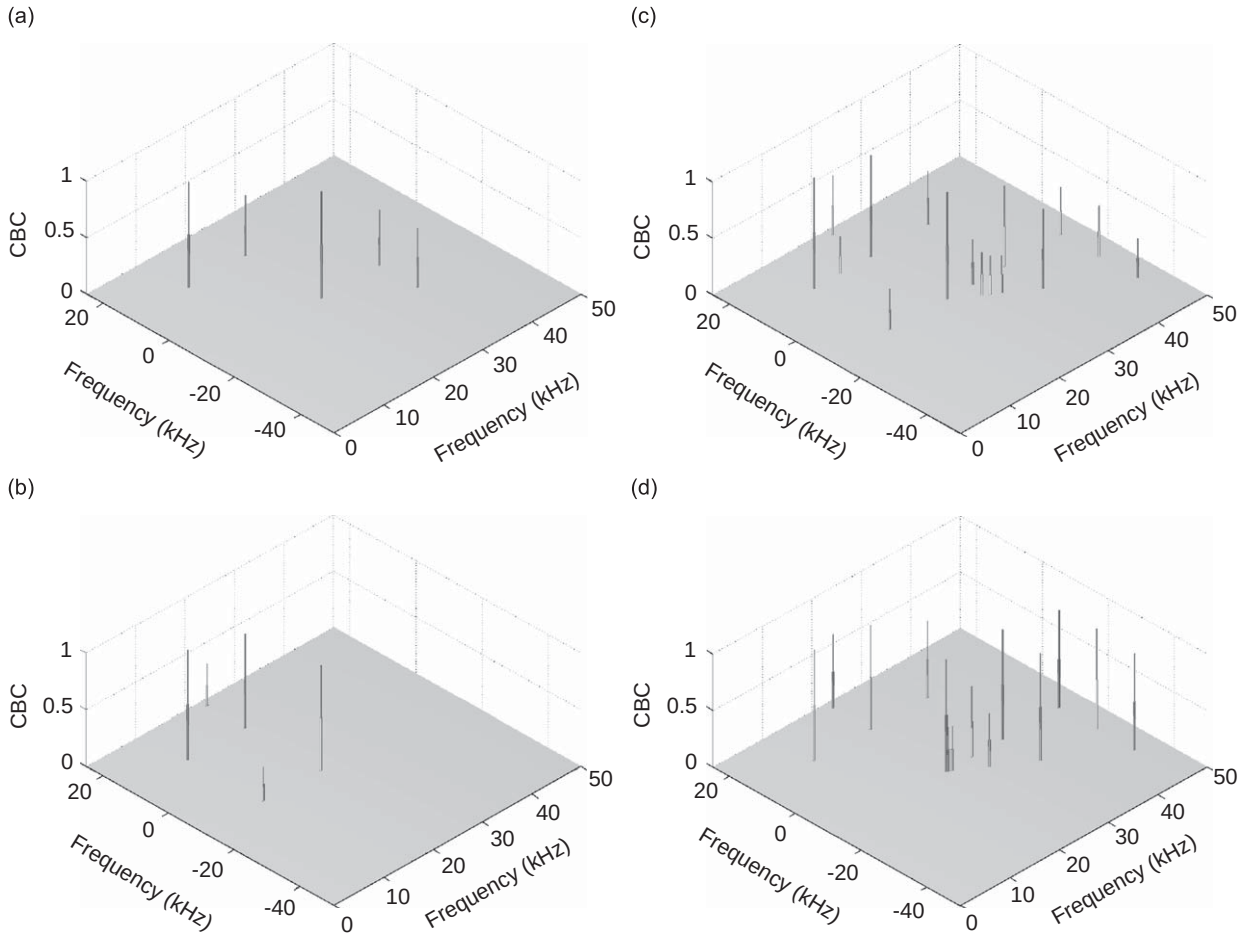

Fig. 14. Cross-bicoherence and spectra of co-directed twin jets at $M_j = 1.46$, for various inter-nozzle spacings. (a) $s/h = 7.3$, (b) $s/h = 7.5$, (c) $s/h = 7.7$, and (d) $s/h = 7.9$.

interactions along horizontal and vertical lines at positions corresponding to the fundamental frequency, marked in Fig. 15 as 'A' and 'B', pointing out the 'most active participating modes'. Furthermore, in most of the cross-bicoherence spectra in Fig. 14, there is a trail of interaction zones tending to form a -45° line in the cross-bicoherence spectrum (marked in Fig. 15 as 'C'), indicating the 'most preferred resultant modes'.

In all these cases, the fundamental frequency seems to be the most desired resultant frequency from the nonlinear interactions. These interactions are classified as 'rectilinearly aligned', or 'lineal' interactions.

3.5. More new metrics defined

In order to view all the observations in a common perspective, two more metrics are introduced. The first, termed as 'Interaction density' (I_c), is the number of peaks in the cross-bicoherence spectrum above a certain threshold value. In this study, threshold values of 0.3, and 0.4 have been used. The threshold is indicated in the subscripts.

Fig. 16 shows the variation of interaction density with Mach number for all the configurations studied, for threshold values of 0.3 and 0.4. Observations made using interaction density are consistent with the earlier discussions, and can be summarized as follows: (i) the interaction density of co-directed twin jets are much higher compared to contra-directed jets, (ii) the single jet displays intermediate values, and (iii) the interaction

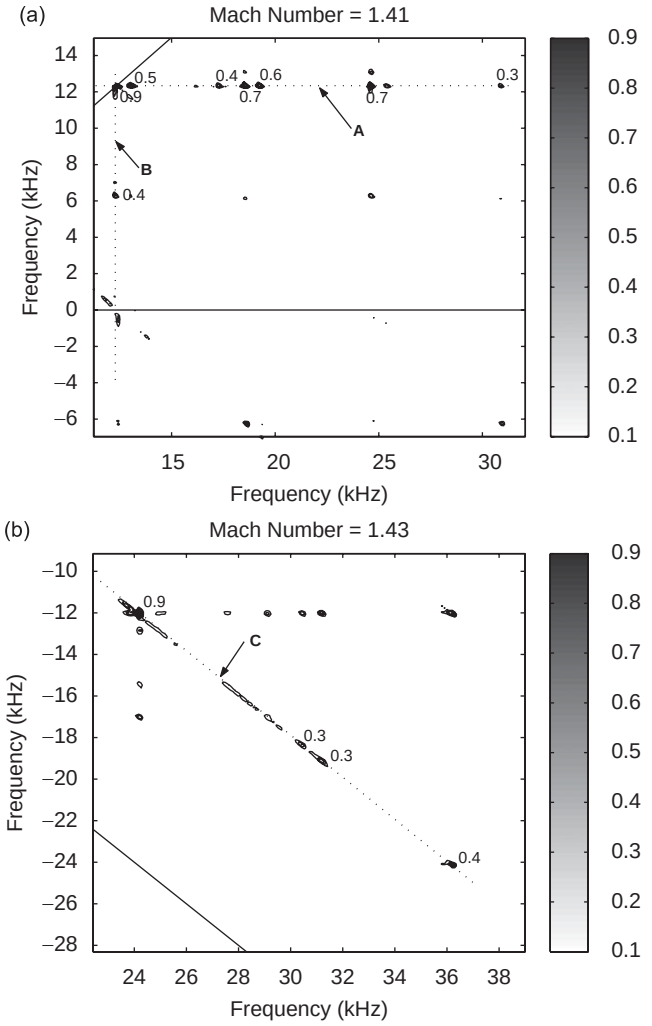

Fig. 15. Close-up views of rectilinearly aligned interactions. (a) Lines 'A' and 'B' denote the actively participating frequencies, and (b) line 'C' indicates the most desired resultant frequency.

density for the co-directed twin jets show a sharp increase around $M_j = 1.4$. This Mach number is the one at which a coupling shift occurred from symmetric to antisymmetric, in our earlier work [28].

The earlier studies had concluded based on linear phase measurements that coupling existed only when the inter-nozzle spacing was $s/h = 7.3$. However, the present results show that nonlinear interactions exist and tend to increase with spacing. This indicates that although there is no evidence of linear coupling at higher spacings, there seems to be a strong nonlinear coupling at higher spacings. It was observed that the behavior of interaction density is the same for the two values of bicoherence threshold considered, which enhances confidence in the new metric developed. To further elucidate the use of this metric, the interaction density is plotted against Mach number and spacing, as shown in Fig. 17. The figures show clearly that I_c peaks near the symmetrically coupled Mach number, and the Mach number where the coupling switched.

In order to consider the effect of inter-nozzle spacing and Mach number on the interaction density, the interaction densities of co-directed twin jets were averaged at each Mach number using four inter-nozzle spacings of $s/h = 7.3$, 7.5, 7.7, and 7.9. The third metric is termed the 'Average Interaction density'. The average interaction densities obtained are plotted against Mach number as shown in Fig. 18(a,b) for cross-bicoherence threshold values of 0.3, and 0.4, respectively. From these plots, it is clear that the nonlinear

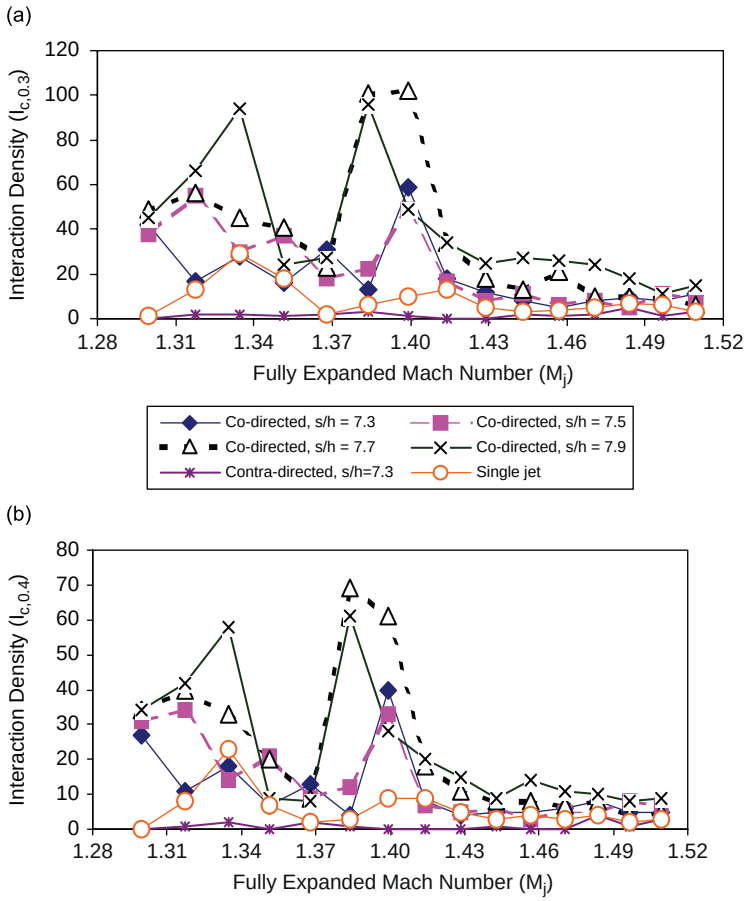

Fig. 16. Interaction density variation with fully expanded jet Mach number, M_j. (a) Threshold 0.3 and (b) threshold 0.4.

interactions sharply increase at around $M_j = 1.4$, where linear phase coherence shows a switch from symmetric to antisymmetric coupling. Thus, it may be conjectured that a coupling mode switch is accompanied by an increase in the extent of interactions. Fig. 18(c,d) show the average interaction densities, calculated by averaging the interaction densities over all Mach numbers for a certain inter-nozzle spacing. These graphs show the effect of inter-nozzle spacing considering the entire Mach number range. The plots show that there is a monotonic increase in the interaction density with inter-nozzle spacing, and the observations are similar for both cross-bicoherence threshold values considered. This corroborates the previous observation that an increase in inter-nozzle spacing promotes nonlinear interactions among the sound sources (up to the maxima location).

It was pointed out in Thomas and Chu [23] that the planar shear layer showed a preference for difference interactions rather than sum interactions. Based on the metrics defined above, the distribution between sum and difference interactions in twin jets was analyzed. Like shear layers, twin jets also seem to prefer difference interactions. It was observed that except for few single jet cases, the difference interactions dominate sum interactions in all the configurations and Mach numbers studied ($I_{c,\mathrm{diff}} > I_{c,\mathrm{sum}}$). The total number of sum and difference interactions, summed over all the test Mach numbers, for various jet configurations have been shown in Table 2. It is clear from this table that difference interactions are almost double the number of sum interactions for all co-directed twin jets. In the case of single jets, the difference interactions outnumber the sum interactions by about 19%. In the case of contra-directed jets, the total number of sum and difference interactions is extremely low; nevertheless the number of difference interactions exceeds that of the sum interactions.

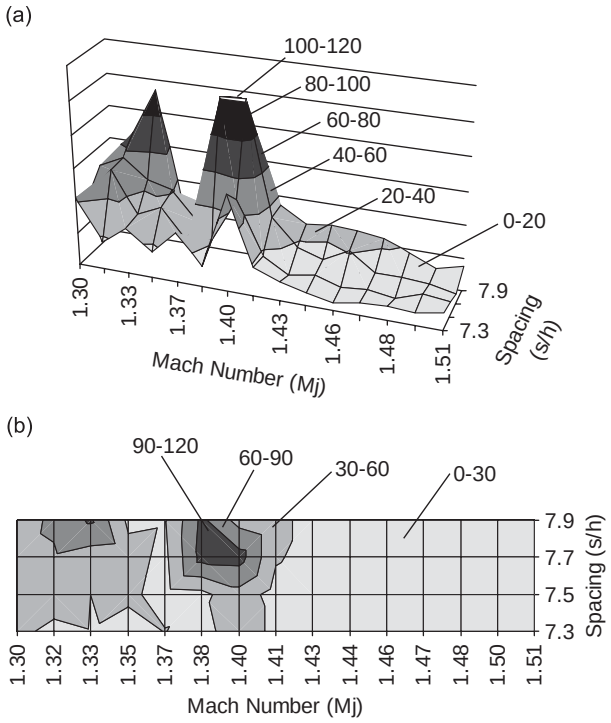

Fig. 17. Interaction density (threshold 0.3) variation with Mach number and spacing. (a) Surface plot and (b) contour plot.

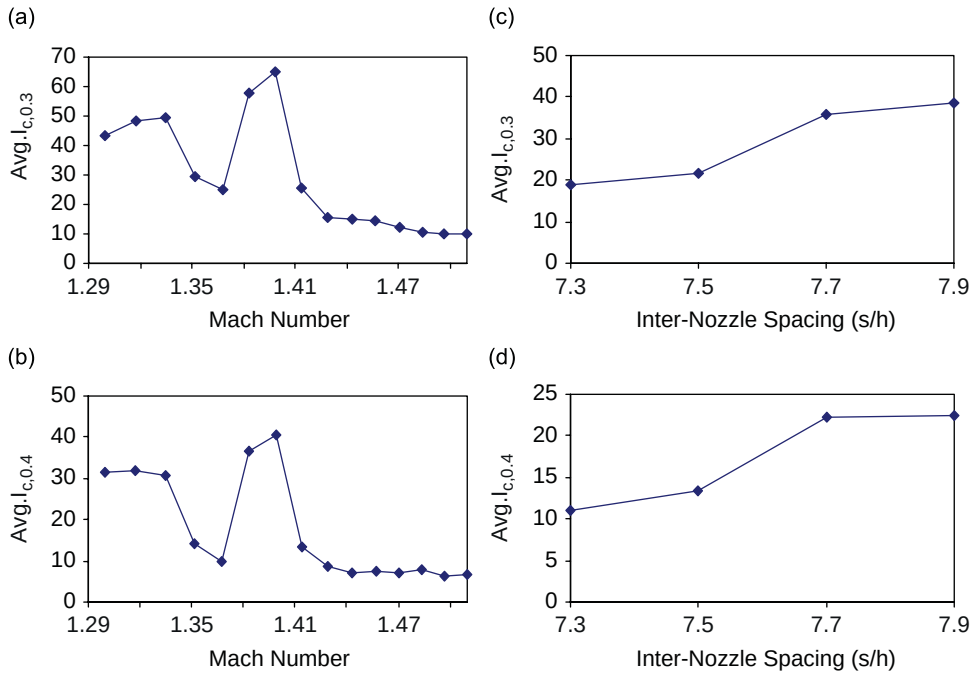

Fig. 18. Variation of average interaction density with Mach number and inter-nozzle spacing. (a,c) Cross-bicoherence threshold 0.3 and (b,d) cross-bicoherence threshold 0.4.

Table 2
Total number of sum and difference interactions summed over all Mach numbers for all the test cases.

No.	Geometry	Total number of sum interactions	Total number of difference interactions
1.	Co-directed twin jets, $s/h = 7.3$	101	184
2.	Co-directed twin jets, $s/h = 7.5$	100	224
3.	Co-directed twin jets, $s/h = 7.7$	169	369
4.	Co-directed twin jets, $s/h = 7.9$	162	429
5.	Single jet	57	68
6.	Contra-directed twin jets	9	16

4. Conclusions

In this paper, twin jet coupling behavior is analyzed using nonlinear spectral analysis. Based on the results, it is concluded that co-directed twin jets apparently uncoupled beyond a certain inter-nozzle spacing using standard spectrum analysis, show nonlinear coupling at higher spacings as revealed by nonlinear spectra. In this direction, a new metric termed *Quadratic Phase Coupling Index* (*QPCI*) has been developed, which quantifies the propensity of jets to couple, provided other conditions are favorable. Two patterns of the cross-bicoherence spectra were observed, one in which an array of closely spaced interactions dominate the spectrum, and the other in which the dots tending to form straight lines appear in the spectrum. The latter case indicated the preference of the fundamental frequency as a participant in the nonlinear interactions, as well as a resultant frequency of the interactions. Another new metric has been defined, termed the *interaction density*, based on the number of peaks in the cross-bicoherence spectrum. The interaction density is a useful parameter to quantify nonlinear coupling, which is strongly related to coupling mode switching, and could be an important parameter in modal transitions. A third metric, the *average interaction density* increased sharply around a Mach number that showed a transition between symmetric to antisymmetric coupling in linear phase coherence studies. Therefore, modal transitions in coupling can be accompanied by a large number of nonlinear interactions. The average interaction density increases monotonically with inter-nozzle spacing for the range of spacings considered in the present study. Difference interactions outnumber sum interactions in almost all the cases studied.

Acknowledgments

This work was funded by the US Air Force Office of Scientific Research (AFOSR) with Dr. John Schmisseur as Program Manager.

The authors also thank the referees for their valuable comments and suggestions that helped to improve the manuscript.

References

[1] T.D. Norum, Screech suppression in supersonic jets, *American Institute of Aeronautics and Astronautics Journal* 21 (1983) 235–240.
[2] D.E. Berndt, Dynamic pressure fluctuations in the inter-nozzle region of a twin-jet nacelle, Society of Automotive Engineers Paper SAE-841540.
[3] R.W. Wlezien, Nozzle geometry effects on supersonic jet interaction, American Institute of Aeronautics and Astronautics Paper 87-2694.
[4] J.M. Seiner, J.C. Manning, M.K. Ponton, Dynamic pressure loads associated with twin supersonic plume resonance, *American Institute of Aeronautics and Astronautics Journal* 26 (1988) 954–960.
[5] P.J. Morris, Instability waves in twin supersonic jets, *Journal of Fluid Mechanics* 220 (1990) 293–307.
[6] L. Shaw, Twin-jet screech suppression, *Journal of Aircraft* 27 (1990) 708–715.
[7] M.K. Ponton, J.M. Seiner, Acoustic study of B helical mode for choked axisymmetric nozzle, *American Institute of Aeronautics and Astronautics Journal* 33 (1995) 413–420.
[8] C.K.W. Tam, J.M. Seiner, Analysis of twin supersonic plume resonance, American Institute of Aeronautics and Astronautics Paper 1987-2695.

[9] G. Raman, E.J. Rice, Instability modes excited by natural screech tones in a supersonic rectangular jet, *Physics of Fluids* 6 (1994) 3999–4008.
[10] G. Raman, Cessation of screech in underexpanded jets, *Journal of Fluid Mechanics* 336 (1997) 69–90.
[11] G. Raman, Coupling of twin supersonic jets of complex geometry, *Journal of Aircraft* 36 (1999) 743–749.
[12] G. Raman, Shock-induced flow resonance in supersonic jets of complex geometry, *Physics of Fluids* 11 (1999) 692–709.
[13] C.K.W. Tam, H. Shen, G. Raman, Screech tones of supersonic jets from bevelled rectangular nozzles, *American Institute of Aeronautics and Astronautics Journal* 35 (1997) 1119–1125.
[14] G. Raman, R.R. Taghavi, Coupling of twin rectangular supersonic jets, *Journal of Fluid Mechanics* 354 (1998) 123–146.
[15] R.R. Taghavi, G. Raman, Interaction of twin rectangular supersonic jets in various congurations, American Society of Mechanical Engineers Paper FEDSM98-5243.
[16] C. Kerechanin, M. Samimy, J.-H. Kim, Effects of nozzle trailing edges on acoustic field of a supersonic rectangular jet, *American Institute of Aeronautics and Astronautics Journal* 39 (2001) 1065–1070.
[17] P.J. Morris, G. Chen, T.R.S. Bhat, A linear shock cell model for jets of arbitrary exit geometry, *Journal of Sound and Vibration* 132 (1989) 199–211.
[18] C.K.W. Tam, N.N. Reddy, Prediction method for broadband shock associated noise from supersonic rectangular jets, *Journal of Aircraft* 33 (1996) 298–303.
[19] G. Raman, R. Taghavi, Resonant interaction of a linear array of supersonic rectangular jets: an experimental study, *Journal of Fluid Mechanics* 309 (1996) 93–111.
[20] G. Raman, Screech tones from rectangular nozzles with spanwise oblique shock-cell structures, *Journal of Fluid Mechanics* 330 (1997) 141–168.
[21] Y.C. Kim, E.J. Powers, Digital bispectral analysis and its applications to nonlinear wave interactions, *IEEE Transactions on Plasma Science* 7 (1979) 120–131.
[22] K.I. Kim, E.J. Powers, A digital method of modeling quadratically nonlinear systems with a general random input, *IEEE Transactions on Acoustics, Speech and Signal Processing* 36 (1988) 1758–1769.
[23] F.O. Thomas, H.C. Chu, Experimental investigation of the nonlinear spectral dynamics of planar jet shear layer transition, *Physics of Fluids (A)* 3 (1991) 1544–1559.
[24] F.O. Thomas, H.C. Chu, Measurement of nonlinear wave coupling and energy transfer in plane jet shear layer transition, American Institute of Aeronautics and Astronautics Paper 1991-0314.
[25] F.O. Thomas, H.C. Chu, Nonlinear wave coupling and subharmonic resonance in planar jet shear layer transition, *Physics of Fluids A* 5 (1993) 630–646.
[26] F.O. Thomas, H.C. Chu, Experiments on the nonlinear stages of excited and natural planar jet shear layer transition, *Experiments in Fluids* 14 (1993) 451–467.
[27] S.H. Walker, F.O. Thomas, Experiments characterizing nonlinear shear layer dynamics in a supersonic rectangular jet undergoing screech, *Physics of Fluids* 9 (1997) 2562–2579.
[28] P. Panickar, K. Srinivasan, G. Raman, Aeroacoustic features of coupled twin jets with spanwise oblique shock-cells, *Journal of Sound and Vibration* 278 (2004) 155–179.